Journal of the Ceramic Society of Japan 128 [8] 518-522 2020
DOI http://doi.org/10.2109/jcersj2.20015

JCS-Japan

FULL PAPER

Control of crystal structure and performance evaluation of multi-piezo material of $Li_{1-x}Na_xNbO_3:Pr^{3+}$

Hirotaka HARA[1,2], Chao-Nan XU[1,2,†], Ruiping WANG[1], Xu-Guang ZHENG[3], Maiko NISHIBORI[2] and Eiji NISHIBORI[4]

[1]National Institute of Advanced Industrial Science and Technology (AIST), Saga 841–0052, Japan
[2]Department of Molecular and Material Sciences, Kyushu University, Fukuoka 816–8580, Japan
[3]Department of Physics, Faculty of Science and Engineering, Saga University, Saga 840–8502, Japan
[4]Division of Physics, Faculty of Pure and Applied Sciences and Tsukuba Research Center for Energy Materials Science, University of Tsukuba, Ibaraki 305–8571, Japan

Piezoelectric $LiNbO_3:Pr^{3+}$ has recently attracted attention as a so-called multi-piezo material, exhibiting simultaneously piezoluminescence and piezoelectricity. In order to investigate and improve the performance of piezoluminescence and piezoelectricity in the newly found multi-piezo material $LiNbO_3:Pr^{3+}$, a systematic study has been carried out on both the crystal structural stability and the correlated multi-piezo performance through structure control between $LiNbO_3$ and $NaNbO_3$. Full set samples of $Li_{1-x}Na_xNbO_3:Pr^{3+}$ ($x = 0$–1) with various Li/Na ratios were synthesized, and the crystal structure, piezoluminescence performance, piezoelectric property d_{33}, and their correlations were systematically investigated. We found that four crystal phases, $LiNbO_3$-*R*3*c*, $NaNbO_3$-*R*3*c*, $NaNbO_3$-*P*2$_1$*ma*, $NaNbO_3$-*Pbma*, can exist stably with co-existence in $Li_{1-x}Na_xNbO_3:Pr^{3+}$ by controlling the Li/Na ratio. A strong correlation between piezoluminescence and piezoelectric properties was verified. Furthermore, the highest piezoluminescence intensity and piezoelectric constant were realized near the phase boundary of $NaNbO_3$-*R*3*c* and $NaNbO_3$-*P*2$_1$*ma*, demonstrating the crystal structure control as a promising technology to engineer multi-piezo materials.

Key-words : Multi-piezo, Mechanoluminescence, $Li_{1-x}Na_xNbO_3$, $LiNbO_3$, Piezoluminescence

[Received January 20, 2020; Accepted May 4, 2020]

1. Introduction

Mechanoluminescence (ML) is the phenomenon of light emission produced by a mechanical stimulus.[1)] Innovative advances in non-destructive ML materials in the elastic deformation are based on the discovery of repeatable ML (also called as piezoluminescence, elastic-ML) in ZnS:Mn^{2+} and $SrAl_2O_4:Eu^{2+}$ by Xu in 1999.[2),3)] Since then, various ML materials, as well as their mechanisms and applications have been reported.[4)–14)] Recently, we discovered a multi-piezo material, which simultaneously generates both piezoluminescence and piezoelectricity, by doping Pr^{3+} into $LiNbO_3$.[15)] The $LiNbO_3$ is a lead free piezoelectric material widely used for sensors, surface acoustic wave (SAW) devices, optical modulators, etc., due to its excellent piezoelectric, nonlinear optical, and electro-optical properties. Therefore, the so-called "multi-piezo" material $LiNbO_3:Pr^{3+}$ is viewed as a promising candidate for realizing innovative devices for multifunctional conversion applications. However, few researches have been carried out on the correlation between the piezoluminescence and piezoelectricity, which is required to elucidate the mechanism of multi-piezo. The piezoluminescence intensity of $LiNbO_3:Pr^{3+}$ multi-piezo material is also insufficient for practical uses.

The ML intensity can be enhanced by controlling the crystal structure of the material. Improving the functional characteristics of a new material by partial substitution of cations is an effective method in the field of phosphors, as well as in the ML materials. It has been reported that the ML in blue mechanoluminescent material $CaAl_2Si_2O_8:Eu^{2+}$ was improved due to a change in the crystal structure when the Ca^{2+} was replaced with Sr^{2+}.[16)] Both piezoelectric and ferroelectric materials exhibit strong electromechanical coupling effects, which are highly dependent on the crystal structure.[17),18)] It is well known that $LiNbO_3$ shows a trigonal ilmenite-like structure stable even at high temperatures up to ca. 1200 °C. However, $Li_{1-x}Na_xNbO_3$, wherein the Li^+ is partially substituted by Na^+, were reported to form a very complicated phase diagram depending on the ratio of Li/Na.[19)–26)] We think that the unusual phase behaviors of $Li_{1-x}Na_xNbO_3$ implies a

† Corresponding author: C. N. Xu; E-mail: cn-xu@aist.go.jp
‡ Preface for this article: DOI http://doi.org/10.2109/jcersj2.128.P8-1

potential to significantly improve the piezoluminescence and piezoelectric properties. The present work systematically investigates the crystal structure, piezoluminescence, and piezoelectric properties of $Li_{1-x}Na_xNbO_3$. It is aimed to improve the multi-piezo performance, and provide systematic data for studying the mechanism of multi-piezo and their correlation.

2. Experimental procedures

All samples were synthesized by a solid-state reaction method. Dried powders of Li_2CO_3 (99.99%), Na_2CO_3 (99.8%), Nb_2O_5 (99.9%) and Pr_2O_3 (99.9%) were mixed according to the nominal composition of $Li_{1.01-x}Na_x$-$Pr_{0.002}NbO_3$ (LNx). The mixture was calcined in an air atmosphere at 650 °C for 5 h, then thoroughly crushed and sintered at 900–1150 °C for 8 h. The crystalline phases of the obtained samples were investigated by a powder X-ray (Cu Kα) diffractometer (RINT2000, Rigaku). The photoluminescence and excitation spectra were measured using a fluorescence spectrophotometer (FP6600, JASCO) equipped with a 150 W Xe lamp. ML properties were evaluated using a standard method according to the following procedure. 1) Cylindrical resin pellet in diameter of 25 mm and thickness of 15 mm was prepared by mixing 0.5 g of a powder sample with 5.0 g of optical epoxy resin. 2) The prepared resin pellet was irradiated with ultraviolet rays of 365 nm for 3 min, then waited for 3 min. 3) Using a material test machine (RTC-1310A, Orientec Corporation) to apply a compressive load with a triangular waveform from 0 to 1000 N at a cross head speed of 3 mm/min. In this experiment, a photomultiplier tube (R645, Hamamatsu Photonics) and a photon counter (C5410, Hamamatsu Photonics); as well as a charge coupled device (CCD) camera (TXG04, Baumer, Radeberg, Germany), were used to measure the piezoluminescence intensity at the center of the pellet. Piezoelectric measurement was performed by using a d_{33} meter (APC International, Ltd., Wide-Range d_{33} Tester) on a high density ceramic pellet, poled at 100 °C under a DC electric field of 55 kV/cm for 30 min.

3. Results and discussion

The typical powder X-ray diffraction (XRD) patterns of the synthesized $Li_{1.001-x}Na_xNbO_3:Pr^{3+}$ (LNx) ($x = 0$–1) were shown in **Fig. 1**(a). All diffraction data from both the laboratory and synchrotron facilities were analyzed by a comprehensive pattern matching for the full composition of LNx ($x = 0$–1) using the crystal structure database of (Li,Na)NbO_3. The reliability for such identification has been confirmed by the results of the ferroelectricity and dielectric properties and Rietveld refinement. Finally, four phases have been identified to be involved in the examined LNx, The first is $LiNbO_3$ of trigonal phase (*R3c*, hereafter Li-*R3c*, ICCD 01-085-2456), the second is $NaNbO_3$ with polar rhombohedral phase (*R3c*, hereafter Na-*R3c* in order to distinguish from the $LiNbO_3$ phase, ICCD 01-085-0396), the third is $NaNbO_3$ with polar orthorhombic phase ($P2_1ma$, ICCD 01-082-0606), and the fourth is $NaNbO_3$ of orthorhombic phase (*Pbma*, ICCD 01-089-8957), as shown in Fig. 1(a) for each diffraction pattern and Fig. 1(b) for the crystal structure.

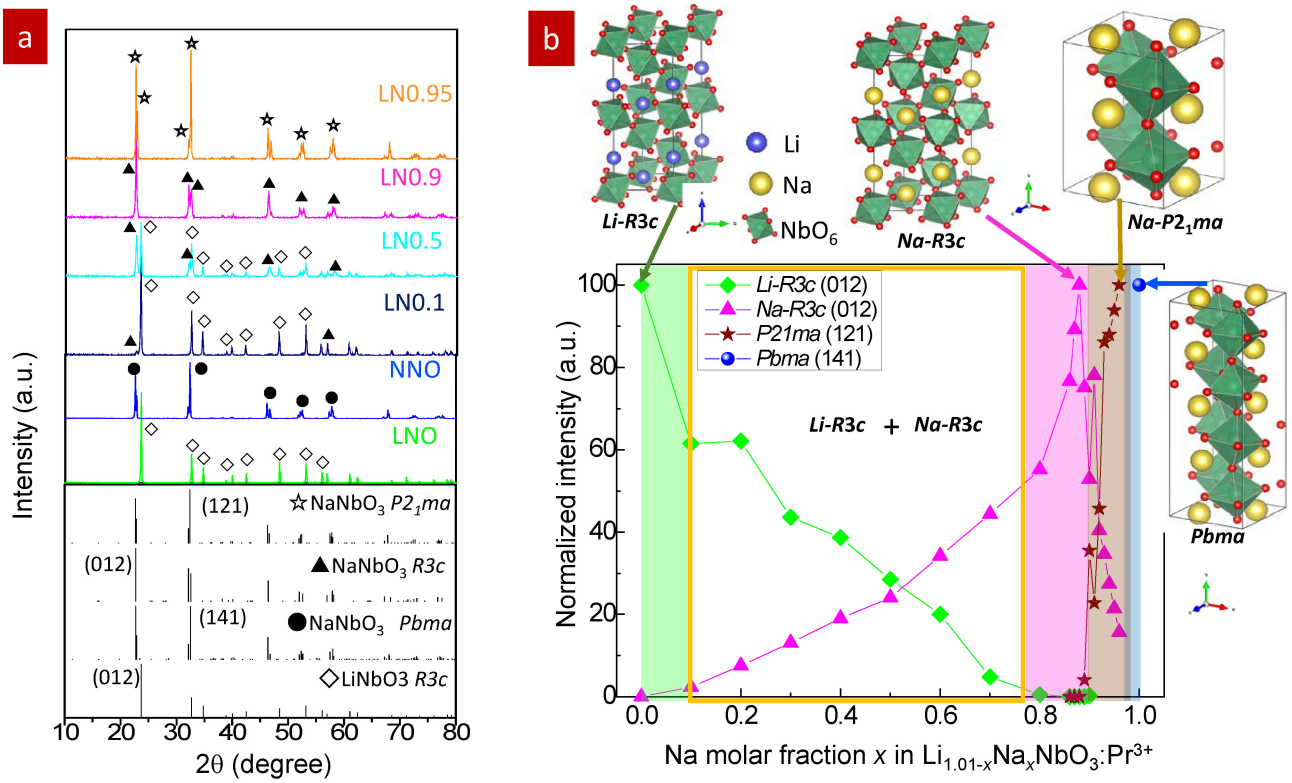

Fig. 1. (a) XRD patterns of four phases confirmed by LNx samples (partially listed $x = 0$, 0.1, 0.5, 0.9, 0.95, 1.0), (b) Dependence of each crystal phase on Na substitution content x.

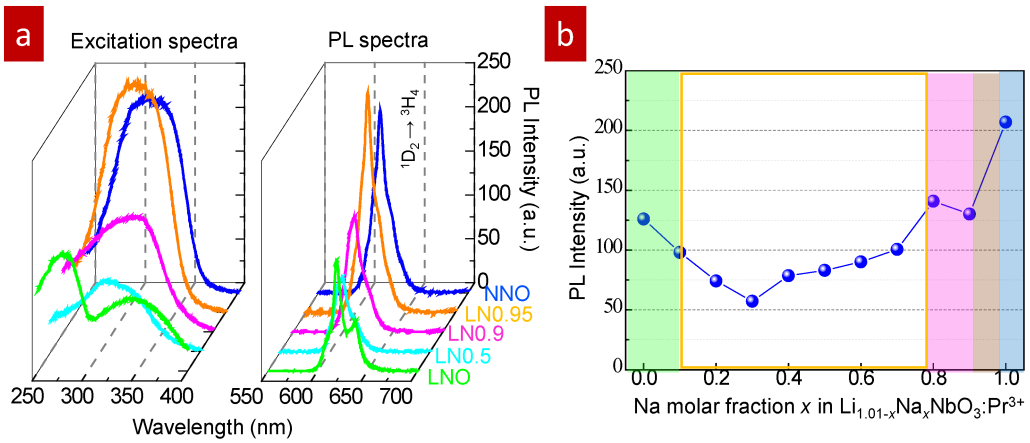

Fig. 2. (a) Excitation spectra and PL spectra of LNO, NNO, and LNx, (b) Dependence of PL intensity on Na substitution content x.

The pure $LiNbO_3:Pr^{3+}$ (LNO, $x = 0$) was identified to be the single phase of rhombohedral (trigonal) in space group $R3c$, whereas the $NaNbO_3:Pr^{3+}$ (NNO, $x = 1$) was found to be the single phase of orthorhombic in space group $Pbma$ in consistency with previous reports.[4),27)] No other peaks originating from the reagents or impurities were recognized. A micro amount of Pr^{3+} was reported to occupy the Li/Na sites in LNO and NNO.[28),29)] The $Pbma$ perovskite structure NNO exhibits anti-ferroelectricity and LNx is known to exhibit very complex phases. However, the present study has successfully controlled the crystal structure of LNx in four stable crystalline phase, as illustrated in Fig. 1. The single phase with most intensive XRD intensities was confirmed in the composition of $x = 0$, 0.88, 0.95, 1.00, for Li-$R3c$, Na-$R3c$, Na-$P21ma$, $Pbma$ crystal structures, respectively. Further confirmation of the analyzed crystal structures was performed by using a synchrotron X-ray experiment at BL02B2, SPring-8. The single phase of Na-$R3c$ at $x = 0.88$ has been confirmed with the lattice parameter of $a = 0.547254$ nm, $c = 1.372509$ nm by Rietveld refinement of the Spring-8 data. The phase volume fraction was approximately estimated by calculating the ratio of each LNx sample value to the XRD intensity of these four samples using the XRD peak at Li $R3c$ (012), Na-$R3c$ (121), $P21ma$ (121) and $Pbma$ (141), as shown in Fig. 1(b). The full composition region of $Li_{1-x}Na_xNbO_3$ synthesized (LNx, $0 \leq x \leq 1.0$) can be conveniently divided into five regions. First, region 1 between $0 \leqq x < 0.1$, in which a single phase of the Li-$R3c$ phase exists, as shown in Fig. 1(b). Second, region 2 between $0.1 \leqq x < 0.8$, in which two phases of the rhombohedral $R3c$ structure were found to co-exist stably. In them, one is a Li-rich phase having the $LiNbO_3$-like structure (referred as Li-$R3c$), and the other one is a Na-rich phase having the $NaNbO_3$-like structure (referred as Na-$R3c$). This Na-$R3c$ structure is known to be the ferroelectric phase structure only stable at low temperatures (<173 K) in pure $NaNbO_3$. In the present study, the Na-$R3c$ structure is confirmed to be stable at high temperatures in LNx, which has a much higher degree of distortion than the perovskite structure of $NaNbO_3$ in the $Pbma$ phase. Contrary to the normal perovskite structure, Li and Na at the A site were viewed as taking 6 coordination instead of 12,[19)] wherein the LiO_6 or NaO_6 octahedron share a face with the NbO_6 octahedron. From the change in the diffraction peak intensities, it can be seen that as the Na substitution amount increases, the phase volume ratio of Na-$R3c$ versus Li-$R3c$ increased prominently. Third, the region 3 between $0.80 \leqq x \leqq 0.90$, wherein Li-$R3c$ cannot be confirmed, and only Na-$R3c$ is present. Forth, the region 4 between $x = 0.91$–0.99 with the formation of ferroelectric orthorhombic $P2_1ma$ (Na-$P2_1ma$) phase appeared, which is consistent with the previous report that the Na-$P2_1ma$ phase could be obtained by doping low amounts of Li^+ or K^+ into $NaNbO_3$.[30)] Finally, the region 5 at $x = 1.0$, wherein the orthorhombic: $Pbma$ phase was confirmed only in pure $NaNbO_3$ composition.

Figure 2 shows the PL spectra for typical samples of LNx. As shown in Fig. 2(a), LNO showed two broad excitation spectra centered at 280 and 350 nm. These two excitation spectra are considered to be due to charge transfer at the oxyanion site.[14)] As Li^+ was substituted by Na^+, the two peaks merged into a broad peak centered at 310 nm. In the PL spectra measurement, luminescence derived from the f–f transition of Pr^{3+} ($^1D_2 \rightarrow {}^3H_4$) was confirmed in all samples. As shown in Fig. 2(b), the PL intensity in the mixed phase region of Li-$R3c$ and Na-$R3c$ was lower than that of pure LNO or the strongest PL intensity in the orthorhombic $Pbma$ NNO. This is probably due to the reduced crystallinity in the mixed phases, which is supported by the lower XRD peak intensity of LN50, as shown in Fig. 1.

Figure 3(a) shows the piezoluminescence response curves of LNx. Compared to LNO, all samples ($0.1 \leqq x \leqq 0.9$) in the rhombohedral structure showed an increase of piezoluminescence intensity in proportion to the load, with LN90 showing the largest value. Figure 3(b) shows the changes in the crystal structure and the piezoluminescence intensity with the amount of Na substitution. The crystal structure was described using the software VESTA.[31)] In the mixed phase region of Li-$R3c$ and Na-$R3c$, the piezoluminescence intensity increases as the ratio of Na-$R3c$

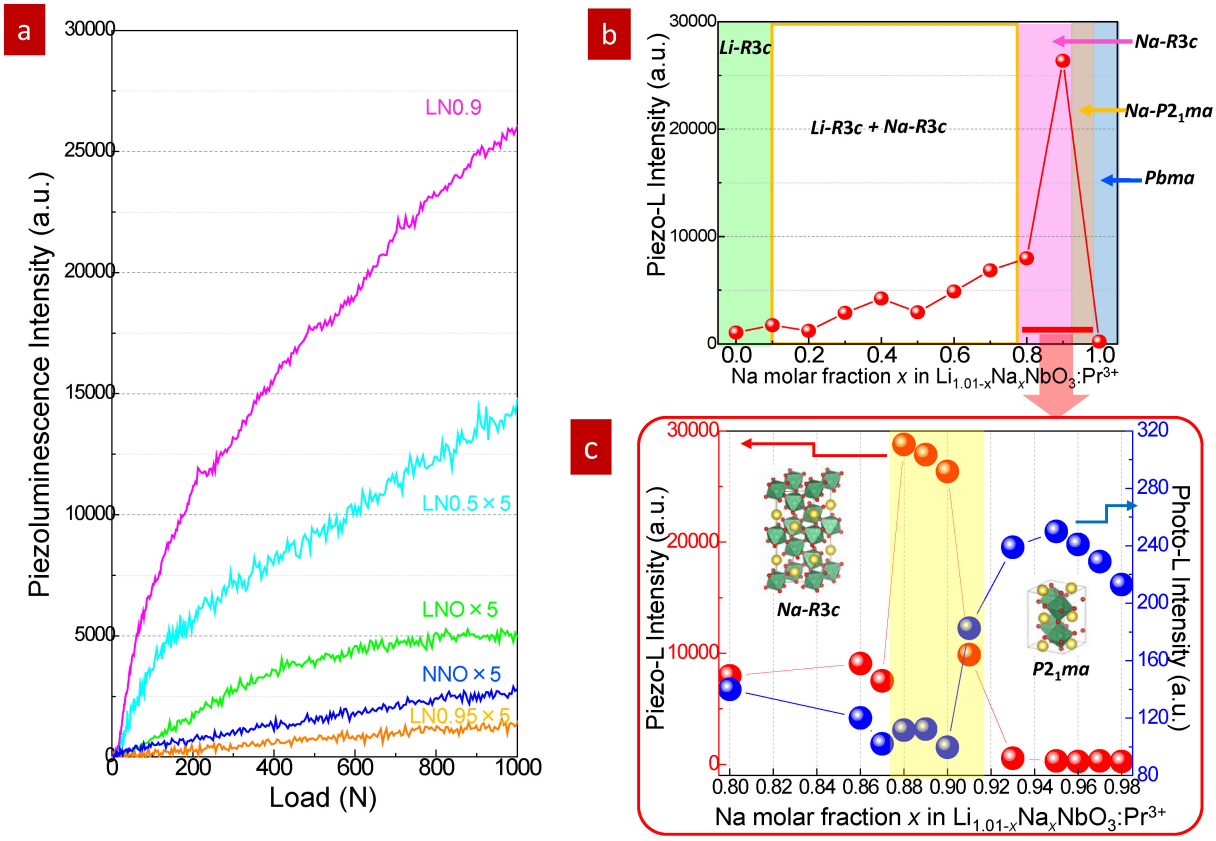

Fig. 3. (a) Piezoluminescence response curves of LNxN samples (partially listed $x = 0.5$, 0.9, 0.95), (b) Transitions of piezoluminescence intensity by Na substitution content x, and inset is the crystal structure of each region, (c) Piezo-L and Photo-L intensity changes near the phase boundary.

increases, suggesting that the *Na-R3c* contributes to piezoluminescence more than *Li-R3c*. Li-*R3c* and Na-*R3c* have different lattice distortions and local structures due to differences in the ionic radius. Such a structure of Na-*R3c* is considered suitable for piezoluminescence materials. The *Na-P2*$_1$*ma* and NNO (*Pbma*) showed strong PL, but only emitted weak piezoluminescence. It is considered that the piezoluminescence decreased due to the phase transition to the orthorhombic system. This is because *P2*$_1$*ma* and *Pbma* have higher crystal symmetry than *R3c*, thus they are not suitable for piezoluminescence materials due to their less-distorted structure. Also, it can be seen that there is a large difference between the piezoluminescence intensity in LN80 and LN90 in the same *Na-R3c* structure. Therefore, we further investigated the piezoluminescence and PL in the range of $x = 0.8$ to 0.95 and observed strong piezoluminescence for $x = 0.88$, 0.89, and 0.90 [Fig. 3(c)]. Conversely, the PL intensity decreases slightly, and then abruptly increases in LN91 where the piezoluminescence intensity begins to dramatically decreases. Referring to the XRD results in **Fig. 4**, we can see that a large increase in piezoluminescence intensity occurs near the phase boundary between *Na-R3c* and *Na-P2*$_1$*ma*, and a small amount of *Na-P2*$_1$*ma* exists in LN90. On the other hand, a complete transformation to the *Na-P2*$_1$*ma* phase drastically reduces piezoluminescence. The piezoluminescence in the $x =$ 0.88, 0.89, 0.90 samples are so strong that they can be

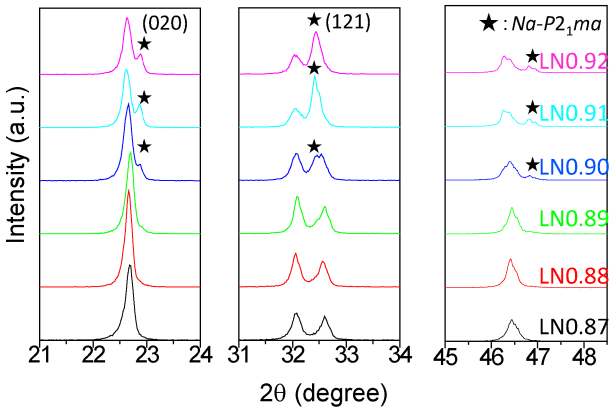

Fig. 4. XRD patterns transitions near the phase boundary.

easily visualized with the naked eyes even in a bright environment, which obviously can be used for stress sensing.

Finally, the comparison of the piezoelectric constant d_{33} and piezoluminescence intensity is shown in **Fig. 5**. The piezoelectric constant increases in correlation with the piezoluminescence intensity in the range where the rhombohedral structure is formed ($0.1 \leqq x \leqq 0.9$). The strongest piezoluminescence and the largest piezoelectric constant were observed at the phase boundary of *Na-R3c* and *P2*$_1$*ma*. As seen from the inset of Fig. 5, there is a close correlation between the piezoelectricity and piezoluminescence.

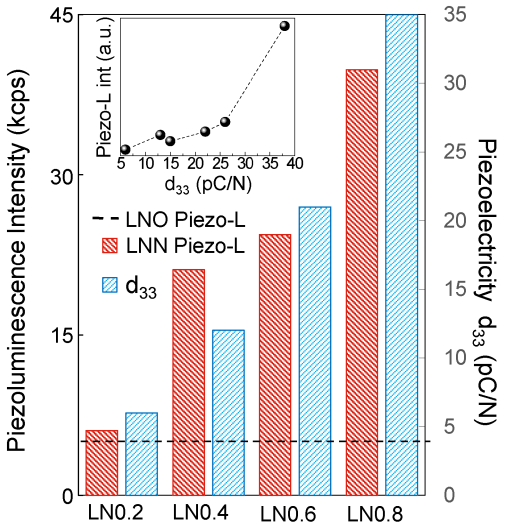

Fig. 5. Correlation between piezoelectric constant d_{33} of LN*x*N and piezoluminescence intensity.

The present work provides unambiguous evidence that controlling the crystal structure by substitution greatly improves the performance of multi-piezo materials.

4. Conclusion

In order to improve the multi-piezo performance (piezoluminescence and piezoelectric) of (Li,Na)NbO_3, we tried an element substitution approach. By substituting Na, four crystal phases were confirmed, and strong piezoluminescence was observed in rhombohedral *Na-R*3*c*. Significant improvement in piezoluminescence was realized near the phase boundary of *Na-R*3*c* and orthorhombic $P2_1ma$, which could be easily confirmed with naked eyes. The piezoelectric constant d_{33} also showed a tendency proportional to the piezoluminescence intensity, suggesting a correlation between piezoelectric and piezoluminescence. Therefore, we have succeeded in improving the multi-piezo performance by controlling the crystal structure, and provided a systematic data for elucidating the mechanism of multi-piezo.

Acknowledgments This research was partially supported by JSPS KAKENHI Grant Numbers 19H00835, 18H04499 and 17H06374. The synchrotron radiation experiments were performed at the BL02B2 of SPring-8 with the approval of the Japan Synchrotron Radiation Research Institute (JASRI) (Proposal No. 2017A1606, 2019A0068). We deeply thank all collaborators for their experimental support and helpful discussion, especially Prof. H. Tateyama, Ms. E. Kawasaki, I. Arima, F. Furusawa. M. Kubo, and Y. Asano at AIST, and H. Kasai, S. Takahashi at the University of Tsukuba.

References

1) X. Wang, C. N. Xu, H. Yamada, K. Nishikubo and X. G. Zheng, *Adv. Mater.*, 17, 1254–1258 (2005).
2) C. N. Xu, T. Watanabe, M. Akiyama and X. G. Zheng, *Appl. Phys. Lett.*, 74, 2414–2416 (1999).
3) C. N. Xu, T. Watanabe, M. Akiyama and X. G. Zheng, *Appl. Phys. Lett.*, 74, 1236–1238 (1999).
4) S. Kamimura, H. Yamada and C. N. Xu, *J. Lumin.*, 132, 526–530 (2012).
5) H. Zhang, H. Yamada, N. Terasaki and C. N. Xu, *Jpn. J. Appl. Phys.*, 48, 04C109 (2009).
6) J. Li, C. N. Xu, D. Tu, X. Chai, X. Wang, L. Liu and E. Kawasaki, *Acta. Mater.*, 145, 462–469 (2018).
7) J. Hao and C. N. Xu, *MRS Bull.*, 43, 965–969 (2018).
8) D. Tu, R. Hamabe and C. N. Xu, *J. Phys. Chem.*, 122, 23307–23311 (2018).
9) S. Kamimura, H. Yamada and C. N. Xu, *Appl. Phys. Lett.*, 101, 09113 (2012).
10) C. N. Xu, H. Yamada, X. S. Wang and X. G. Zheng, *Appl. Phys. Lett.*, 84, 3040–3042 (2004).
11) C. N. Xu, X. G. Zheng, M. Akiyama, K. Nonaka and T. Watanabe, *Appl. Phys. Lett.*, 76, 179–181 (2000).
12) C. N. Xu, et al., "Mechanoluminescence and Novel Structure Health Diagnosis", NTS Inc. 3-12 (2012).
13) L. Liu, C. N. Xu, A. Yoshida, D. Tu, N. Ueno and S. Kainuma, *Adv. Mater. Technol.*, 4, 1800336 (2019).
14) J. C. Zhang, X. Wang, G. Marriott and C. N. Xu, *Prog. Mater. Sci.*, 103, 687–742 (2019).
15) D. Tu, C. N. Xu, A. Yoshida, M. Fujihala, J. Hirotsu and X. G. Zheng, *Adv. Mater.*, 29, 1606904 (2017).
16) L. Zhang, C. N. Xu, H. Yamada and N. Bu, *J. Electrochem. Soc.*, 157, J50–J53 (2010).
17) Y. Guo, M. Gu, H. Luo, Y. Liu and R. L. Withers, *Phys. Rev. B*, 83, 054118 (2011).
18) J. Wang, Y. Liu, R. L. Withers, A. Studer, Q. Li, L. Norén and Y. Guo, *J. Appl. Phys.*, 110, 084114 (2011).
19) M. D. Peel, S. E. Ashbrook and P. Lightfoot, *Inorg. Chem.*, 52, 8872–8880 (2013).
20) C. A. L. Dixon and P. Lightfoot, *Phys. Rev. B*, 97, 224105 (2018).
21) S. K. Mishra, P. S. R. Krishna, A. B. Shinde, V. B. Jayakrishnan, R. Mittal, P. U. Sastry and S. L. Chaplot, *J. Appl. Phys.*, 118, 094101 (2015).
22) R. M. Henson, R. R. Zeyfang and K. V. Kiehl, *J. Am. Ceram. Soc.*, 60, 15–17 (1977).
23) C. L. Wang, P. L. Zhang, W. L. Zhong and H. S. Zhao, *J. Appl. Phys.*, 69, 2522–2524 (1991).
24) K. Konieczny and P. Czaja, *Arch. Metall. Mater.*, 62, 539–544 (2017).
25) R. Aoyagi, A. Takeda, M. Iwata, M. Maeda, T. Nishida and T. Shiosaki, *Jpn. J. Appl. Phys.*, 47, 7689–7692 (2008).
26) R. Aoyagi, M. Iwata and M. Maeda, *Key Eng. Mat.*, 388, 233–236 (2009).
27) A. M. Glazer and H. D. Megaw, *Acta Crystallogr. A*, 29, 489–495 (1973).
28) A. Lorenzo, H. Jaffrezic, B. Roux, G. Boulon and J. Garcia-Sole, *Appl. Phys. Lett.*, 67, 3735–3737 (1995).
29) P. Boutinaud, *J. Phys. Condens. Matter*, 21, 025901 (2009).
30) M. Ahtee and A. M. Glazer, *Acta Crystallogr. A*, 32, 434–446 (1976).
31) K. Momma and F. Izumi, *J. Appl. Crystallogr.*, 44, 1272–1276 (2011).